

### **TASK III: Development of an Effective Computational Methodology for Body Force Representation of High-speed Rotor 37**

#### **Summary**

A framework for an effective computational methodology for characterizing the stability and the impact of distortion in high-speed multi-stage compressor is being developed. The methodology consists of using a few isolated-blade row Navier-Stokes solutions for each blade row to construct a body force database. The purpose of the body force database is to replace each blade row in a multi-stage compressor by a body force distribution to produce same pressure rise and flow turning. To do this, each body force database is generated in such a way that it can respond to the changes in local flow conditions. Once the database is generated, no further Navier-Stokes computations are necessary. The process is repeated for every blade row in the multi-stage compressor. The body forces are then embedded as source terms in an Euler solver. The method is developed to have the capability to compute the performance in a flow that has radial as well as circumferential non-uniformity with a length scale larger than a blade pitch; thus it can potentially be used to characterize the stability of a compressor under design. It is these two latter features as well as the accompanying procedure to obtain the body force representation that distinguish the present methodology from the streamline curvature method.

The overall computational procedures have been developed. A dimensional analysis was carried out to determine the local flow conditions for parameterizing the magnitudes of the local body force representation of blade rows. An Euler solver was modified to embed the body forces as source terms.

The results from the dimensional analysis show that the body forces can be parameterized in terms of the two relative flow angles, the relative Mach number, and the Reynolds number. For flow in a high-speed transonic blade row, they can be parameterized in terms of the local relative Mach number alone. It is deduced that the performance and the flow distribution of a single blade row subjected to radial inlet distortions can be predicted

using the body force database created from the Navier-Stokes solutions with uniform inlet conditions. Likewise, the performance at an operating point, other than those from which the database for the body forces were extracted, can be computed as well.

## 1. Introduction

Gong [1], as described in Task I above, had developed a model for simulating axial compressor stall inception associated with both long- and short-wavelength disturbances. Individual blade rows were represented by a body force distribution formulated in terms of the blade's pressure rise and flow turning characteristics. The computational model uses a body force distribution that responds to local flow conditions. To achieve this, knowledge about the compressor performance and geometry must be known prior to modeling. The implication of Gong's work is that current thinking on stability modeling by viewing a compressor blade row as a body force distribution appears adequate for situations that have been examined. Such a representation was also determined to be adequate in a separate collaborative research involving NASA GRC, Boeing Commercial Airplane Company, Pratt & Whitney and MIT to incorporate Gong's formulation into WIND code for simulating the aerodynamic coupling between inlet flow and high speed fan stage in high bypass engine for advanced subsonic transport. This was implemented successfully and the work has been published (Hsiao, et al [2001]). Despite the success, there is a need to develop a rational and rigorous procedure for generating body force representation of compressor blade from CFD solutions. Task III essentially constitutes a step taken towards developing such a methodology.

In the past, the body force representation was based on correlation and meanline analysis as was implemented in streamline curvature and throughflow methods in implicit terms. However, the present proposed methodology, to be described later, explicitly obtains the body force representation of each blade row in a multi-stage compressor from the "best" available three-dimensional Navier-Stokes solver on a physically consistent basis.

Whereas a streamline curvature method or throughflow analysis is only capable of computing turbomachinery performance in a flow with radial flow variations, the technical framework under which the present proposed methodology is implemented in such that it can compute the performance in a flow that has radial as well as circumferential variations (with length-scales larger than the blade pitch). As such, it can

be used to characterize the stability of a compressor under design. It is these two latter aspects, namely how body force representation of a blade row is constructed and the ability to deal with a flow with circumferential non-uniformities, that distinguish the present method from the others.

Thus the overall goal is to first develop the methodology for extracting body force representation of blade row from computed flow field based on the best available Navier-Stokes solver. This is then to be followed by applying the methodology to the following practical situations:

- (1) Effect of inlet distortion on high-speed axial compressor performance and stability margin
- (2) Response of high-speed axial compressor to various distribution of jet actuation in the tip region
- (3) Inlet-engine interactions in propulsion system representative of JSF types

This report is organized as follows. The main ideas associated with the body force formulation are first illustrated by the presentation of the physical concepts and the development of a basic computational model. New capabilities added to the existing model are assessed and validated. Specifically, the applicability of the model is first assessed by an extraction of the appropriate body force representation of an isolated blade row and subsequently by a successful replication of the flow field by applying the new representation. Having accomplished the first step, a dimensional analysis is carried out to identify a set of local flow parameters that set the magnitudes of the forces. The use of this set of the local flow parameters for correlating the response of the body forces with respect to the changes in local flow conditions is illustrated for a blade row subjected to a non-uniform inlet flow.

Finally, key results from the development and application of the computational methodology are presented and suggestions for future work are delineated.

## **2. Development Of Computational Methodology**

### **2.1 Body Force Formulation**

As was alluded to in the introduction, the first part of the computational methodology consists body force formulation. A simple graphical representation is shown in Figure 2.1. Figure 2.1(a) represents a conventional CFD approach, e.g. three-dimensional Navier-Stokes analysis, to compute the flow in a blade row. Figure 2.1(b) shows the axisymmetric Euler approach with the basic body force representation to produce the identical flow turning and total-pressure rise: the effects of the blade geometries are replaced by equivalent local body forces. Figure 2.2 illustrates the body force methodology in a three-dimensional view. At each point within the blade row, the body forces can conveniently be described in terms of their three components:  $F_x$ ,  $F_\theta$ ,  $F_r$ , i.e. the axial, tangential, and radial forces, respectively, or a component normal to the flow and a component parallel to the flow.

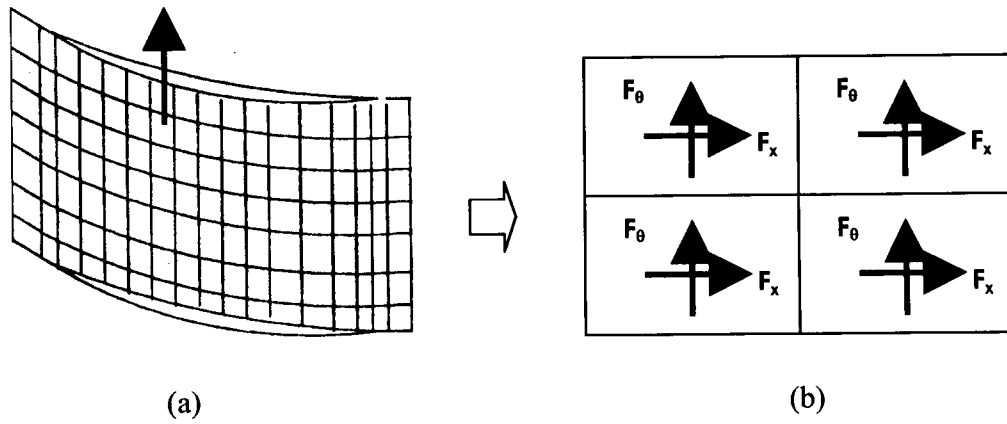


Figure 2.1: Computational methodology: (a) conventional CFD approach and (b) axisymmetric Euler with body force approach

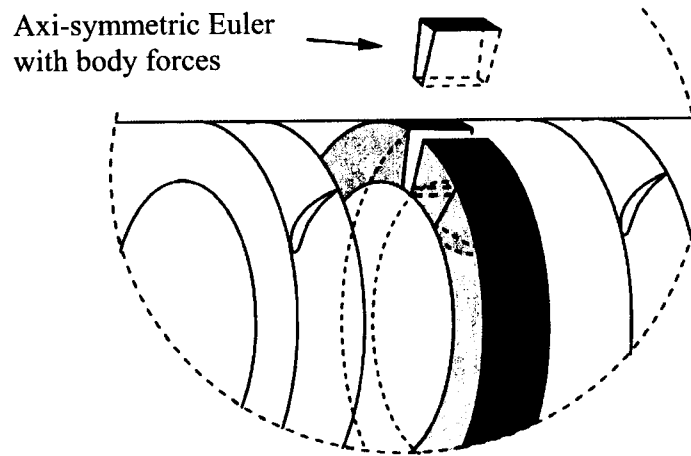


Figure 2.2: Three-dimensional illustration of the model using the body force distributions [8]

## **2.2 Overall Computational Procedure**

The overall computational procedures can be summarized in two flow charts: one for validating the basic body force concept (Figure 2.3) and the other for calculating the compressor performance using the appropriate body force database (Figure 2.4).

### **2.2.1 Procedure for Concept Validation**

A Navier-Stokes solver is used to obtain detailed three-dimensional flow solutions at a mass flow for a given isolated blade row. From the solutions, body forces are extracted by solving the integral form of the momentum equations around the control volumes. The extracted body forces are then substituted as source terms in an Euler flow solver. For the validation step, an Euler computation is performed with the inflow and outflow boundary conditions used to obtain the Navier-Stokes solutions from which the body forces were extracted. The Euler solutions provide one- and two-dimensional mass- and area-averaged profiles of flow variables at various cross sections along the axial direction, as well as the compressor pressure rise to compare against the Navier-Stokes solutions.

### **2.2.2 Procedure for Flow Analysis with a Body Force Database**

The procedure for practical applications involves two steps. The first step consists of generating a body force database for a given blade row (or a set of blade rows). This step is illustrated graphically in Figure 2.4. A Navier-Stokes solver is first used to compute detailed flow fields at various mass flows on a constant speed-line. From the Navier-Stokes solutions, a body force database is constructed. Once the database is available, no further Navier-Stokes computations are required. This step is performed for each blade-row in a multi-stage compressor. Using the body force database, the response of the compressor under different inflow boundary conditions are carried out using the axisymmetric Euler solver. Having specified the inflow and outflow boundary conditions of interest, the solver computes the appropriate local flow conditions. The local flow conditions are fed into the database to update the local body forces and the associated flow

field. This step is repeated until the solution reaches an equilibrium state( Figure 2.5).

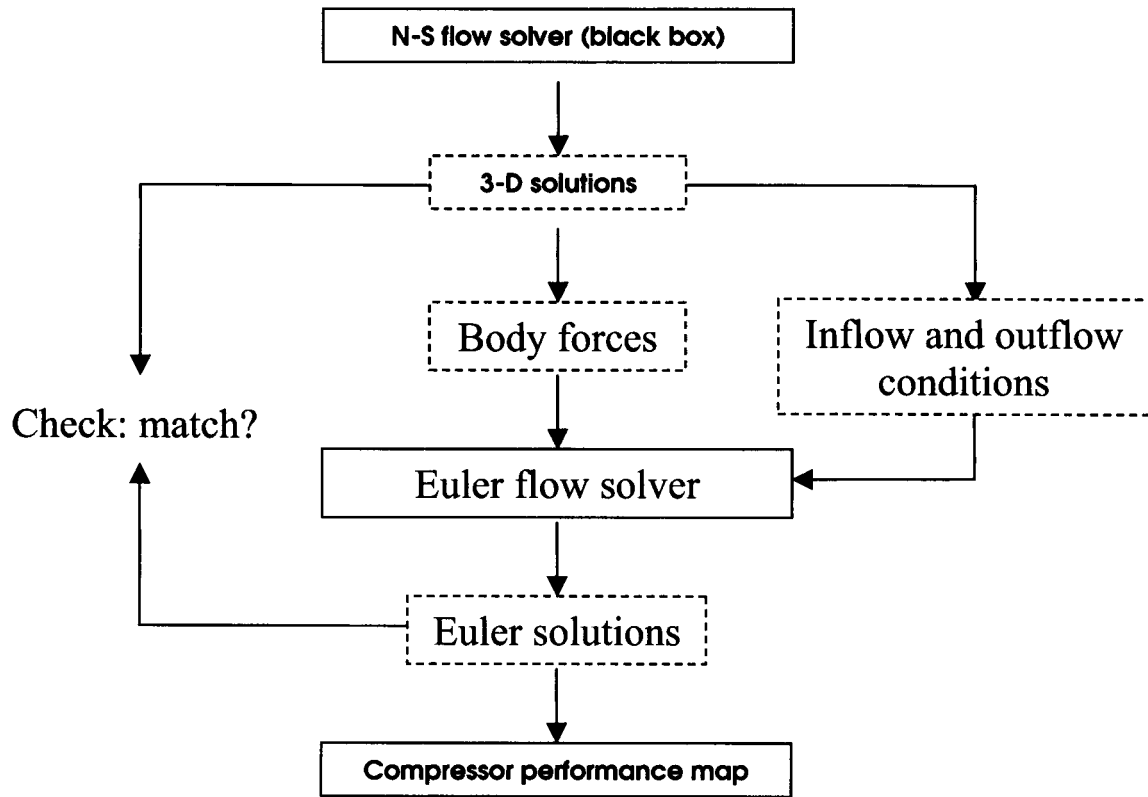


Figure 2.3: Computational methodology for the concept validation

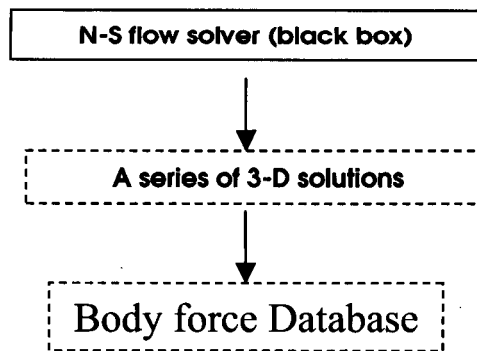


Figure 2.4: Generation of a body force database

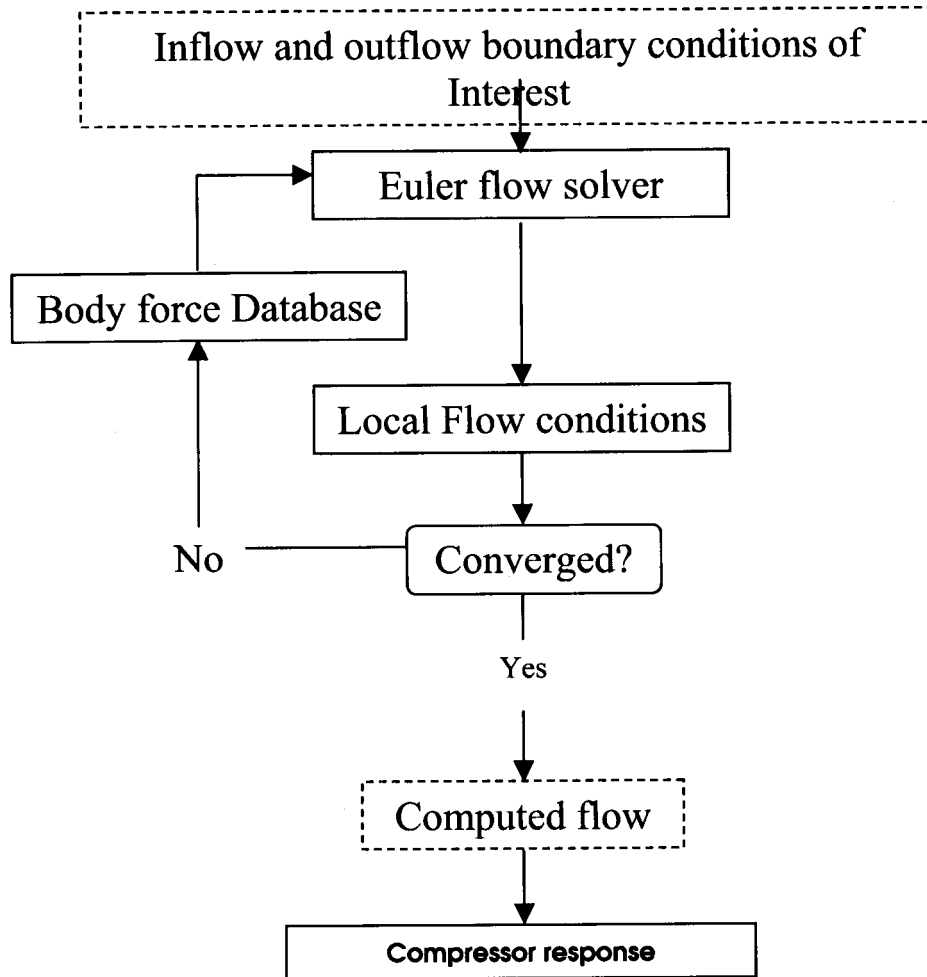


Figure 2.5: Computational procedure for compressor map generation

## **2.3 Generation of Body-Force Database**

The generation of the body force database and its subsequent use to compute compressor response to varying flow conditions underpin the practical applicability of the methodology. In this section we describe the steps to accomplish this. These consist of (1) generating the body force data base, and (2) identifying the local flow conditions which can be employed to parameterize the forces.

### **2.3.1 Parametric Representation of Body Forces**

Computing compressor performance for a new operating point is achievable if the body forces are capable of responding to the changes in the inflow and outflow boundary as well as the operating conditions. The changes in the inflow and outflow boundary conditions include that in radial total pressure, total temperature, axial, and/or tangential velocity profiles in the upstream region, and/or exit static pressure profile in the downstream region of the blade row.

Since those changes usually dictate the changes in the local flow conditions in the blade row, one of the main goal of the parameterization is to enable the body-forces to respond to the changes in the local flow conditions rather than the boundary or operating conditions. To determine what those local flow conditions are, a dimensional analysis using the  $\Pi$ -Theorem has been implemented implemented.

#### **2.3.1.1 Dimensional Analysis**

The first part of the dimensional analysis consists of identifying all the possible independent variables in the governing equations of interest. In this case, the governing equations of interest are the Navier-Stokes equations. Assuming the body forces can be written in terms of some unknown functions of the independent variables of the Navier-

Stokes equations in cylindrical coordinates in the relative frame, the following three equations can be obtained:

$$\begin{aligned} F_x &= f_x(\rho, [V_x]_R, [V_r]_R, [V_\theta]_R, p, \mu, r) \\ F_\theta &= f_\theta(\rho, [V_x]_R, [V_r]_R, [V_\theta]_R, p, \mu, r) \\ F_r &= f_r(\rho, [V_x]_R, [V_r]_R, [V_\theta]_R, p, \mu, r) \end{aligned} \quad (1)$$

where in the left hand side,  $F_x$ ,  $F_\theta$ , and  $F_r$  denote the axial, tangential, and radial forces per unit mass, respectively. The physical quantities in the right hand side are the independent variables in the governing equations. Namely, they are density, three velocity components, static pressure, dynamic viscosity, and the radius (or any other appropriate characteristic length of the blade), respectively. The subscript R in Equations 1 denotes the relative frame of reference.

Since Equation 1 share the common variables, they can be written in terms of a vector form by first defining the body-force vector as follows:

$$\bar{F} = [F_x \quad F_\theta \quad F_r]^T \quad (2).$$

Using Equation 2, Equations 1 can be rewritten as

$$\bar{F} = \bar{f}(\rho, V_x, V_r, V_\theta, p, \mu, r) \quad (3)$$

Applying the  $\Pi$ -Theorem to Equation 3 produces the following functional relationship:

$$\frac{r\bar{F}}{U_R^2} = \bar{f}(\alpha_r, \alpha_\theta, M_R, Re_R) \quad (4)$$

where  $U_R$  is the magnitude of the local relative velocity. Equation 4 implies that the non-dimensional form of the body forces is a function of the following dimensionless

variables: relative radial and tangential flow angle, relative Mach number, and the Reynolds number.

### 2.3.1.2 Subsonic Flows

In general, the relative flow angles in Equation 4 should always be considered for the subsonic flow regime: conceptually, the body forces are proportional to the relative flow angles. This statement is also supported by Gong's work [1]. If the compressibility effect is significant, the relative Mach number should also be included to reflect the effect, in addition to the relative flow angles. In other words, the functional form now becomes

$$\frac{r\bar{F}}{U_R^2} = \bar{f}(\alpha_r, \alpha_\theta, M_R) \quad (5)$$

If the Reynolds number is considerably low, then the Reynolds number must be included as well, i.e.

$$\frac{r\bar{F}}{U_R^2} = \bar{f}(\alpha_r, \alpha_\theta, M_R, Re_R) \quad (6)$$

### 2.3.1.3 Supersonic Flows

For supersonic flows, however, it was found that the relative flow angles could be neglected: the shock waves within the blade passage determine and fix the downstream flow angles. Given the inflow and metal angles, the downstream flow angles can be analytically estimated by using the shock theory. The computed local flow angles from the Navier-Stokes solutions in this flow regime show that their magnitudes do not change at all, although the body forces change noticeably. Therefore, it is concluded that for the supersonic flows, the non-dimensional form of the body forces can be parameterized as:

$$\frac{r\bar{F}}{U_R^2} = \bar{f}(M_R) \quad (7)$$

For the high Reynolds number flow considered here, the Reynolds number dependence can be neglected. That is, the only local flow condition required to parameterize the body forces is the local relative Mach number. In high-speed (transonic) blade rows, Equation 7 is used for the parameterization.

### **2.3.2 Generation Procedure**

#### **2.3.3**

Having identified the local relative Mach number as the sole local flow quantity by which the magnitudes of the body forces at each point in the blade row region can be estimated in the supersonic flow regime, a general procedure adapted to generate a consistent body-force database will be demonstrated here.

To generate the database, several Navier-Stokes solutions of a blade row for various mass flows on a constant speed-line are required in order to estimate the governing relationships between the relative Mach number and the body forces. The solutions from an adequate number of mass flows are necessary to generate the database. To estimate the body force components between any two points along the speed-line, an interpolation scheme was employed.

## **3. Results and Discussions**

Computed results from three examples based on NASA Rotor 37 are presented in this section to validate the computational methodology and to demonstrate its applications. The NASA Rotor 37 is a high-speed research compressor with a high-pressure ratio. It was developed and tested by the NASA in late 1970s as a part of their research program on evaluating the overall performance characteristics of four single stages, i.e. Rotors 35, 36, 37, and 38, that are representative of inlet, middle, and rear stages of an eight-stage 20:1 pressure ratio core compressor.

The rotor has an aspect ratio of 1.19, with an inlet hub-tip ratio of 0.7. It was designed for a total pressure ratio of 2.106 at a mass flow of 20.20 kilograms per second, with the inlet rotor-tip speed of 455 meters per second. In experimental test at design speed, however, the total pressure ratio across the rotor was determined to be 2.056, with an efficiency of 0.876, and actual mass flow rate of 20.74 kilograms per second.

The original configuration of the experimental hardware testing performed by the NASA was a single-stage compressor consisting of a rotor blade row followed by a stator blade row. However, in the current work, the stator blade row was not computationally modeled.

These three examples would serve to demonstrate the capability of the computational methodology (1) to replicate a flow field from which the body forces are extracted, (2) to respond to non-uniform radial inlet distortions using a body force representation that responds to local flow conditions, and (3) to predict the compressor performance at a completely new operating point, of which mass flow is located within the range of the body force database.

### **3.1 Validation of Procedural Steps of Methodology**

In the first example, the body forces were extracted from the Navier-Stokes solutions at one operating point at the design speed and directly substituted in the blade row region in an Euler computation to reproduce the same flow field by matching the mass flow.

The main goal of the test case was simply to illustrate that the body forces can be substituted for the effects of the blade row. The redistribution capability of the body forces was examined in the remaining two examples.

To construct the body forces in the blade row, steady state Navier-Stokes solutions that correspond to 98% design mass flow of the compressor and its grid domain were obtained. The Navier-Stokes solutions were post-processed first to determine the operating and boundary conditions and to understand the overall flow characteristics of the compressor.

The boundary conditions obtained were then used for the Euler computations performed later in the process. These same pre-processing steps were taken for all the examples presented here.

### 3.1.1 Computational Results

Computed results based on Euler Solver with body force representation of rotor 37 were post-processed to obtain the axial variation of the pressure, the temperature rise (both total and static), and the velocity components. These are assessed and compared against those from the Navier-Stokes solutions, and they are shown in Figure 3.1.

The axial velocity and static pressure at each axial location were obtained by using area-averaging technique to conserve mass flow and axial force, respectively. The mass-averaging technique was used for all other variables. The static pressure in the region near the trailing edge of the blade was over-predicted by approximately 5.5 % of the static pressure computed from the Navier-Stokes solutions. Also, it was under-predicted in the upstream region by 5 % of that from the Navier-Stokes solutions. This caused a higher axial velocity in the region also by about 5 % of the axial velocity computed from the Navier-Stokes solutions. However, the two important flow quantities, total-pressure rise and tangential velocity representing the flow turning show excellent agreements. In general, the profiles demonstrate good agreements between the Navier-Stokes and Euler solutions.

Two-dimensional radial profiles at three different axial locations were also generated from both the Euler and Navier-Stokes solutions for comparisons and assessments. As shown in Figure 3.2, the three locations correspond to cross sections at two grid points prior to the leading edge, mid-chord, and two grid points after the trailing edge. The two-dimensional profiles at two grid points prior to the leading edge shown in Figure 3.3 are in good agreement. Matching the upstream conditions ensures that the body forces in the blade region would encounter similar flow conditions as given by the Navier-Stokes solutions. The profiles at the mid chord section in Figure 3.4 indicate that the flow quantities appear to evolve in a manner to yield the same amount of blade work being

added into the flow, as should be. Likewise, the comparisons of the profiles at the cross section after the trailing edge shown in Figure 3.5 show a similar trend.

The radial profiles near the end-walls in Figures 3.3, 3.4, and 3.6 show minor inconsistencies between the Euler and Navier-Stokes solutions. There are two main reasons for these. The first is that the shear forces near the end-walls in the upstream region were not modeled, causing a mismatch of the profiles near the end-walls prior to the leading edge. Since the flow conditions near the end-walls at this section are not identical, all subsequent downstream profiles near the end-walls would not be matched. This discrepancy can be corrected through the use of an appropriate shear force distribution on the hub and shroud. The second could be due to the fact that an Euler solver using different wall boundary conditions was employed to obtain the solutions. The differences had altered the profiles near and on the wall boundaries. The comparison of the pressure rise characteristics at the given operating point in Figure 3.7 also shows excellent agreement. The present results show that the use of an Euler solver with an embedded body force representation of a blade row yields a flow and blade-row performance in accord with that given by the Navier-Stokes solutions.

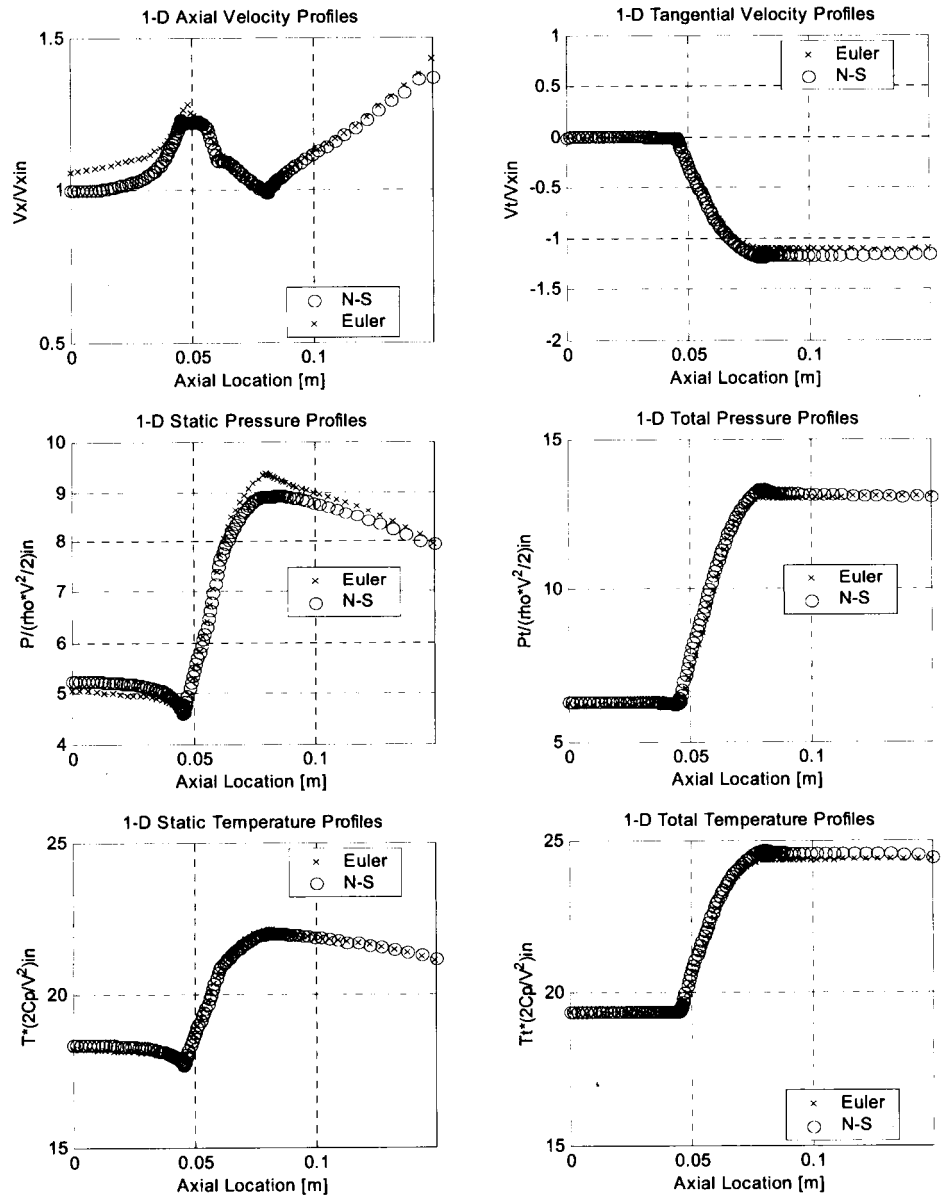


Figure 3.1: Comparisons of one-dimensional profiles of averaged flow solutions. All quantities are mass averaged except axial velocity and static pressure for which area-averaging technique was used.

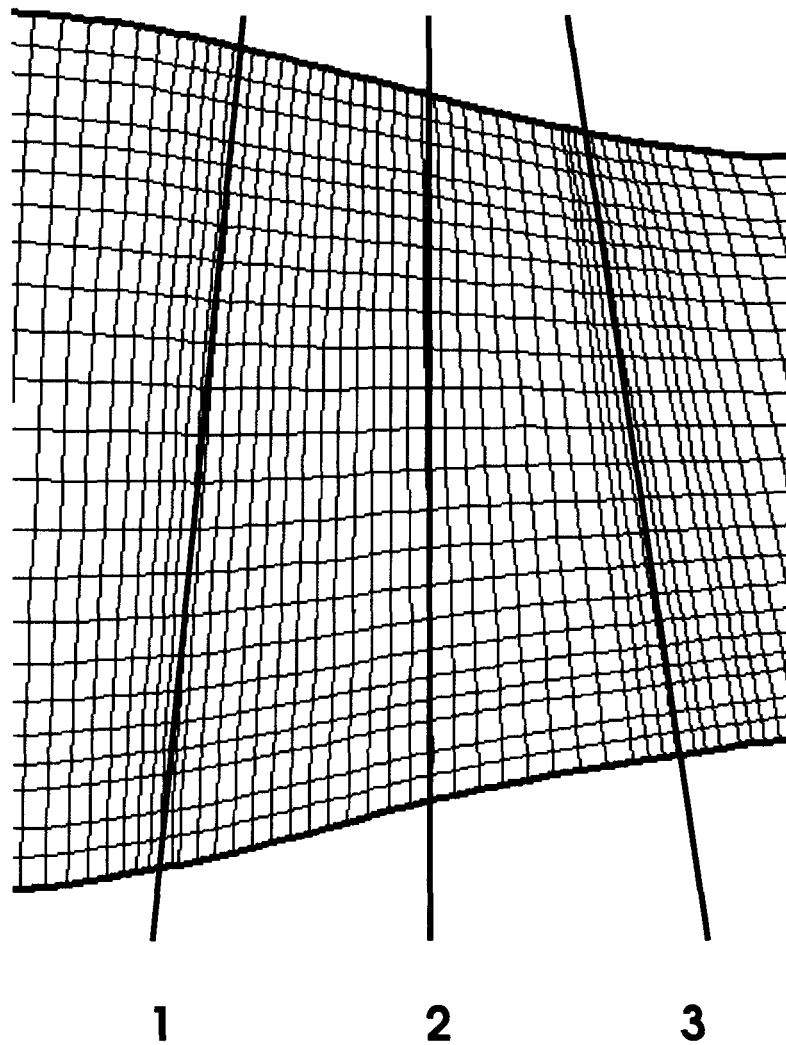


Figure 3.2: Illustration of cross sections chosen for comparisons of two-dimensional radial profiles: (1) two grid points prior to the leading edge, (2) mid-chord, and (3) two grid points after the trailing edge

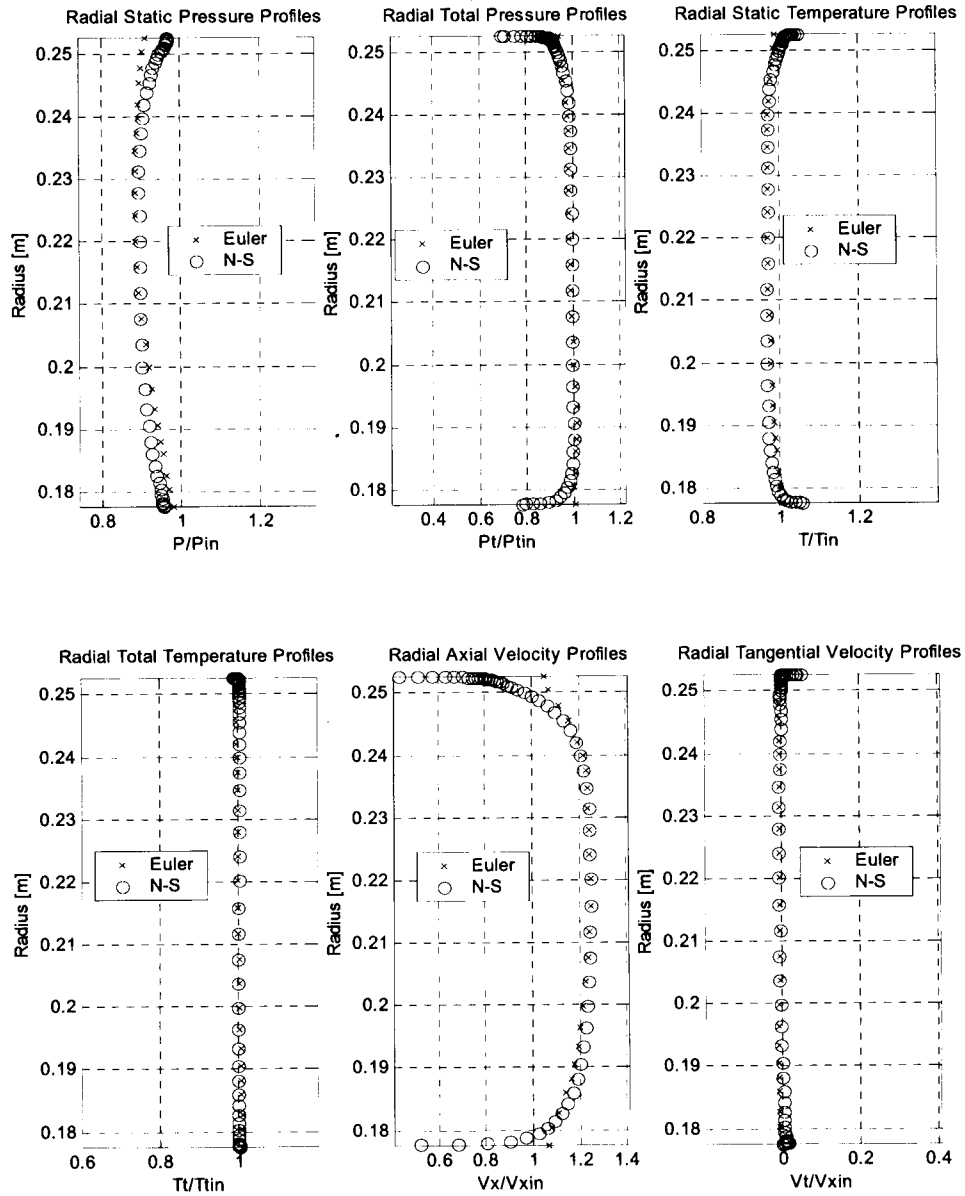


Figure 3.3: Comparisons of radial profiles prior to the leading edge from the first test case

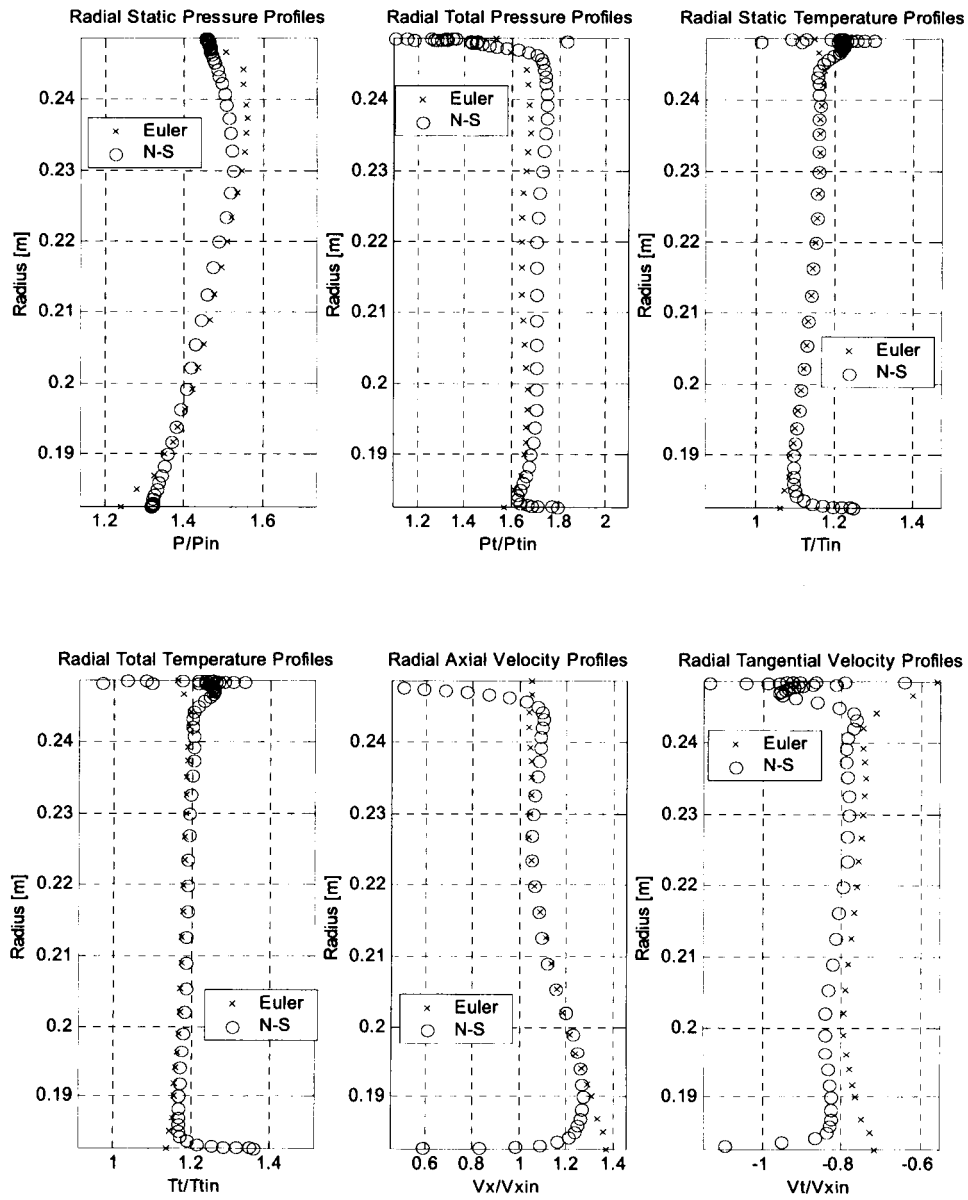


Figure 3.4: Comparisons of radial profiles at the mid-chord from the first test case

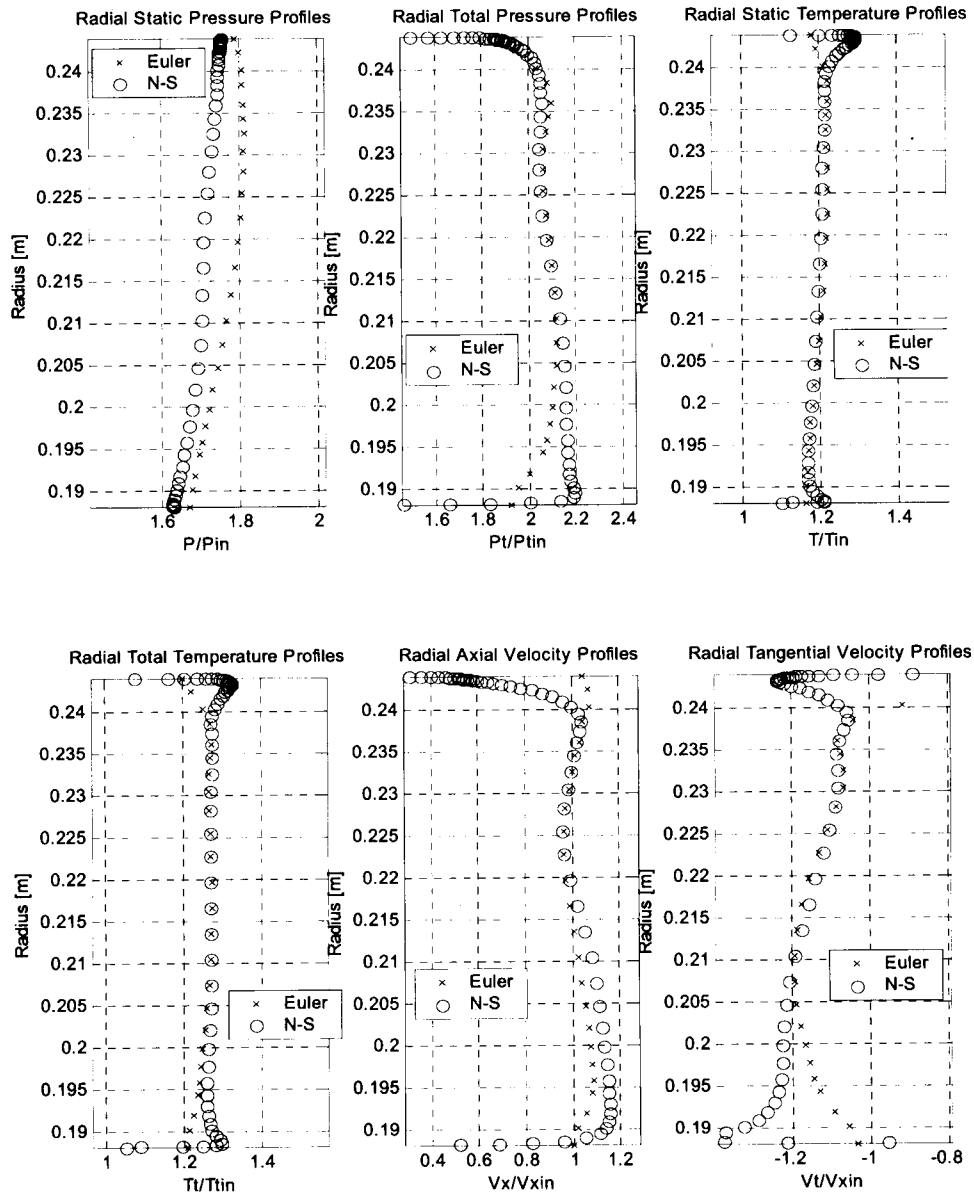


Figure 3.5: Comparisons of radial profiles after the trailing edge from the first test case

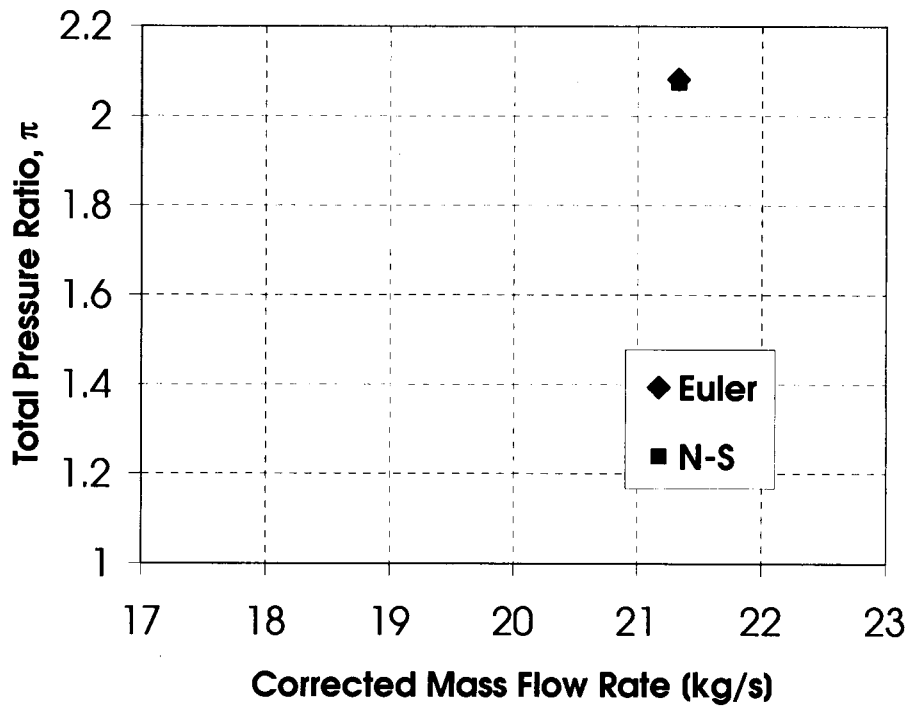


Figure 3.6: Comparisons of pressure-rise characteristics from the first test case

### **3.2 Redistribution of Body forces**

In the second example, a body force database was generated by adapting the procedures described in the above. The local relative Mach numbers in the blade row region were used as the controlling parameter to determine the magnitudes of the body forces. The resulting database contains three relative Mach numbers and their corresponding body force components for each computational cell in the body force grid system.

Using the body force database generated, the replication of operating point 4, shown in Figure 3.7, was first selected for further validating the applicability of the approach. Inflow and outflow boundary conditions constructed from the Navier-Stokes solutions at this operating point were used to compute the flow field. One- and two-dimensional profiles obtained from the computed flow field are presented in Figures 3.8, 3.9, 3.10, and 3.11.

The averaged one-dimensional profiles in Figure 3.8 show good agreements. All the flow quantities obtained from the Euler solutions except the axial velocity profile exhibit no major deviations from that of the original Navier-Stokes solutions. Nevertheless, the axial velocity profiles for this test case are considerably well matched compared to the first test case.

From the comparisons of the two-dimensional profiles, it is deduced that the relative Mach number is indeed adequate to redistribute the body forces in the supersonic flow regime. This deduction is based on the excellent agreements shown in Figures 3.9, 3.10, and 3.11. However, mismatches in the tangential velocity profiles at the mid chord and after the trailing edge indicate that the amount of work added to the flow near the end-wall boundaries may not be quite accurate. This discrepancy was also observed in the first example. The suggestion put forward should resolve this discrepancy observed in the end walls.

Two additional Euler computations were carried out to simulate the pressure-rise characteristics of the rotor at operating points 3 and 5 using the computed flow at point 4 as initial conditions. These operating points are denoted in Figure 3.7. Detailed one- and two-dimensional profiles obtained from the computed flow at the two additional operating points are not shown here as there are no noticeable differences.

Instead, pressure-rise characteristics computed from the Euler solutions are compared against that from the Navier-Stokes solutions for all three operating points; these are presented in Figure 3.12. The figure shows that the pressure-rise characteristics were well predicted with a maximum discrepancy of approximately 2.3 % of the peak pressure rise. From this comparison, it can be concluded that the computational methodology developed in the current work is capable of redistributing the body forces on a consistent basis.

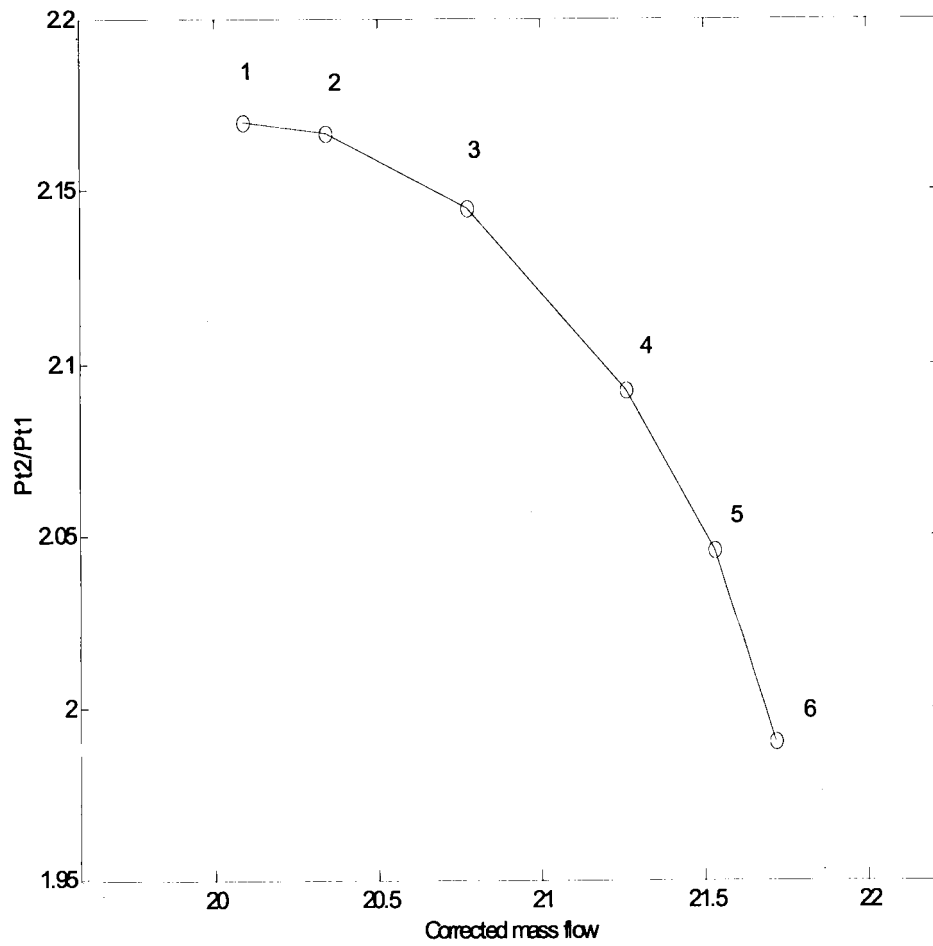


Figure 3.7: Computed Pressure-rise characteristic curve of NASA Rotor 37 on its design speed-line

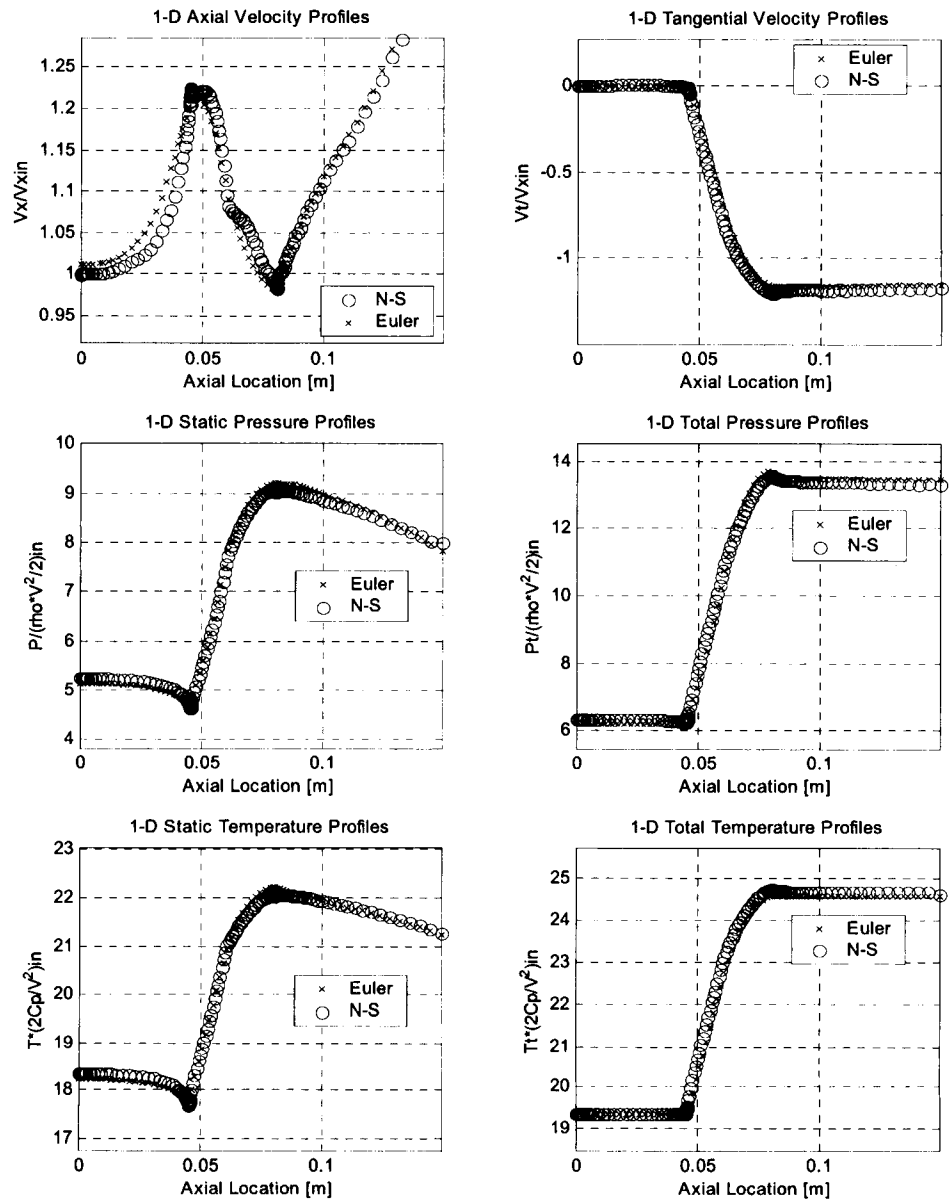


Figure 3.8: Comparisons of one-dimensional profiles of averaged flow solutions from the operating point number 4. All quantities are mass averaged except axial velocity and static pressure for which area-averaging technique was used.

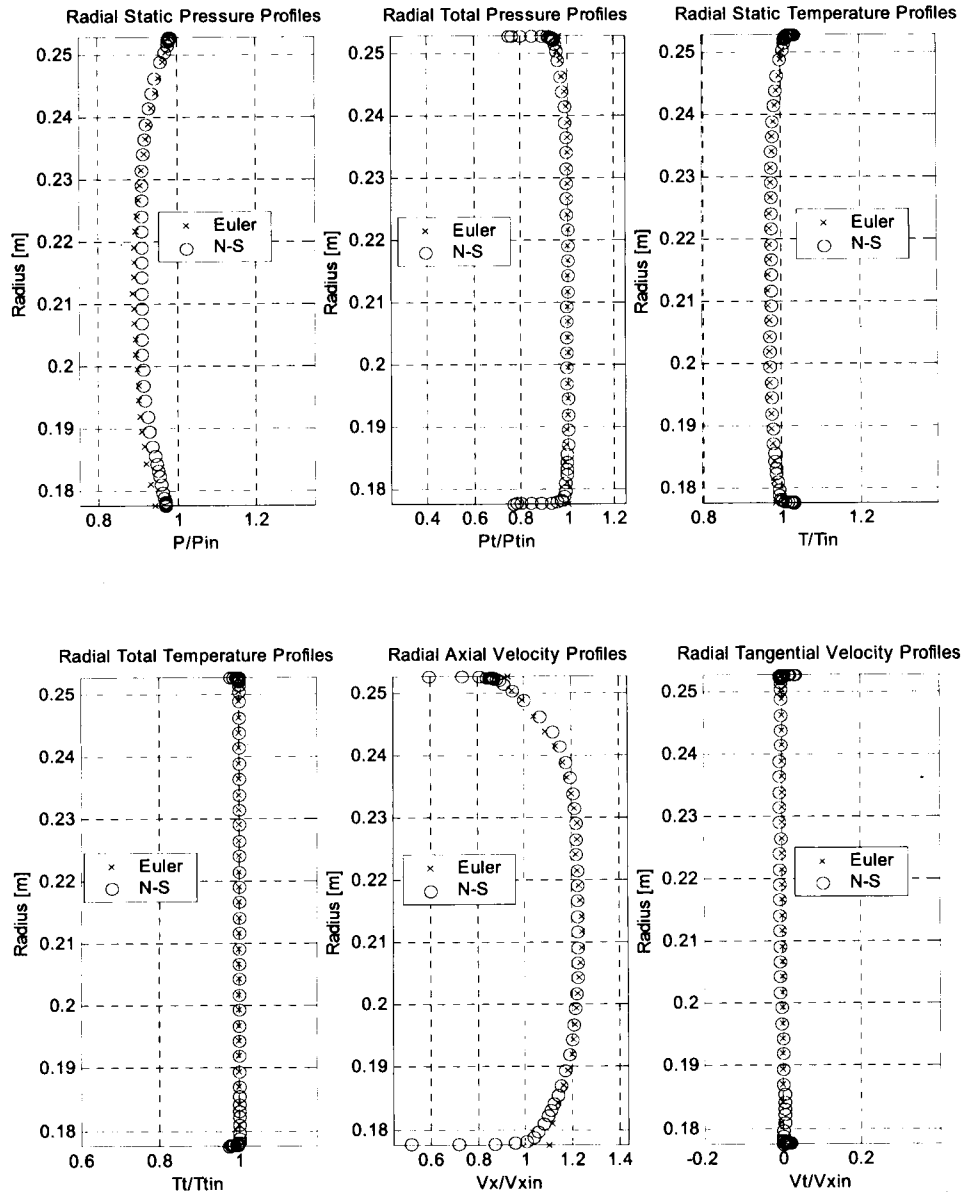


Figure 3.9: Comparisons of radial profiles prior to the leading edge from operating point 4

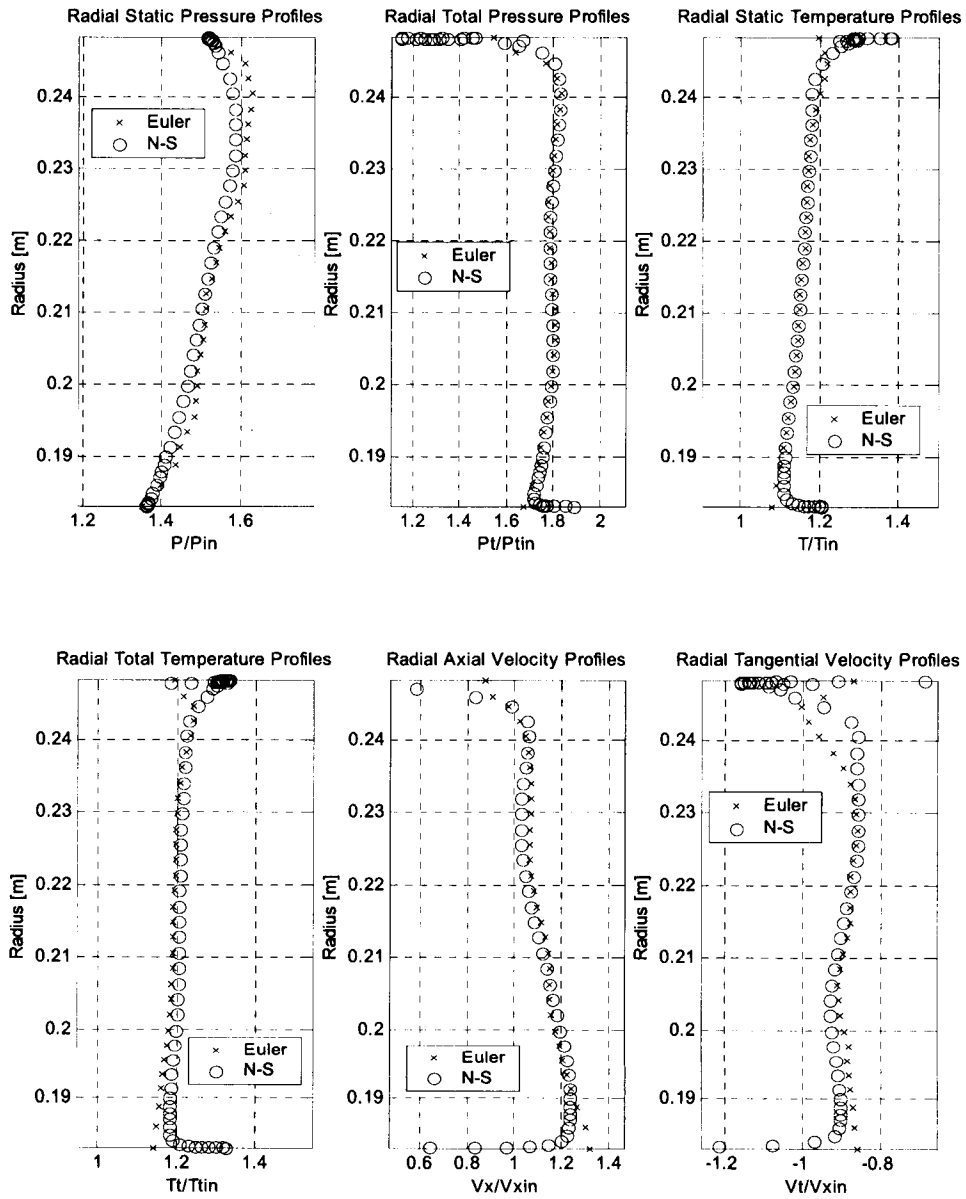


Figure 3.10: Comparisons of radial profiles at the mid-chord from operating point 4

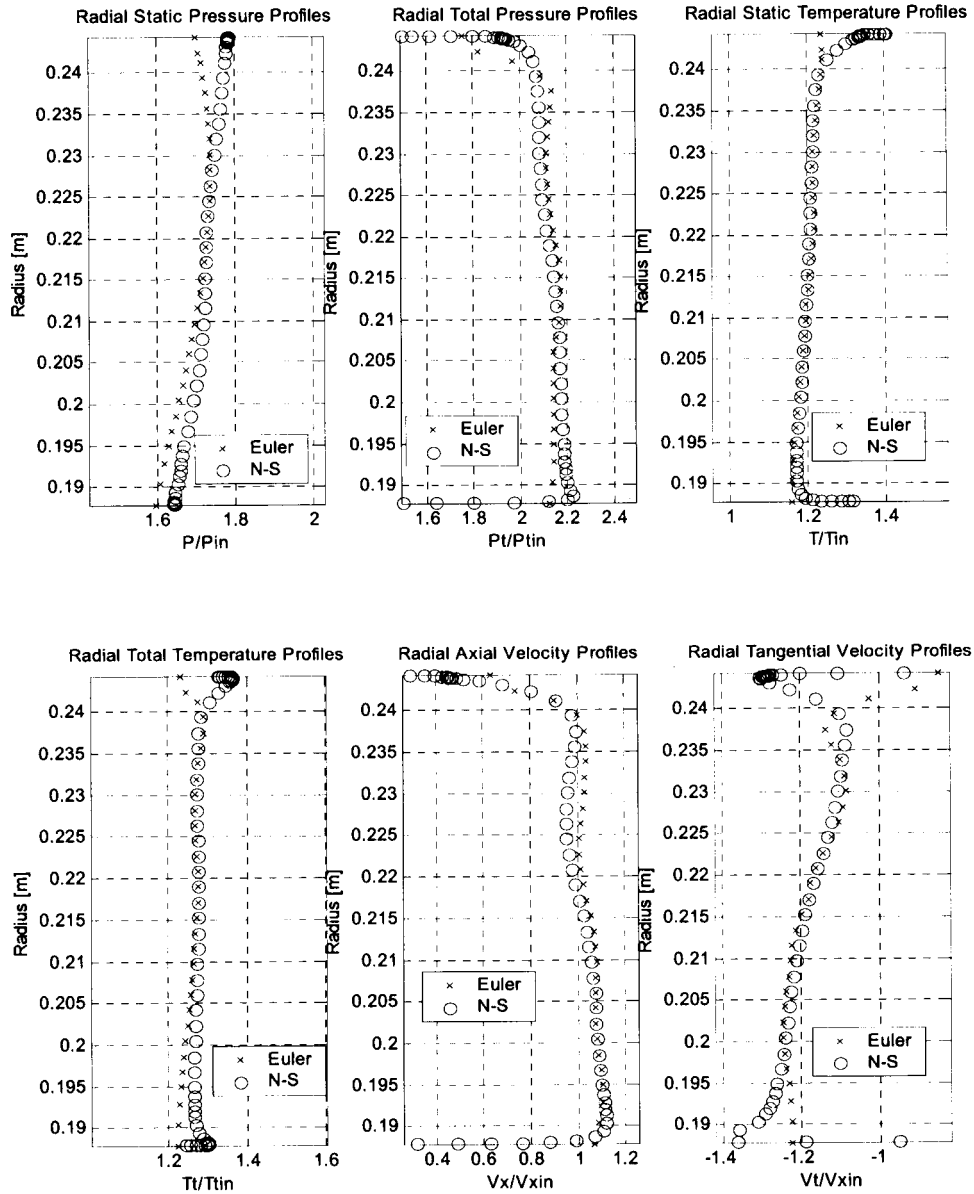


Figure 3.11: Comparisons of radial profiles after the trailing edge from operating point 4

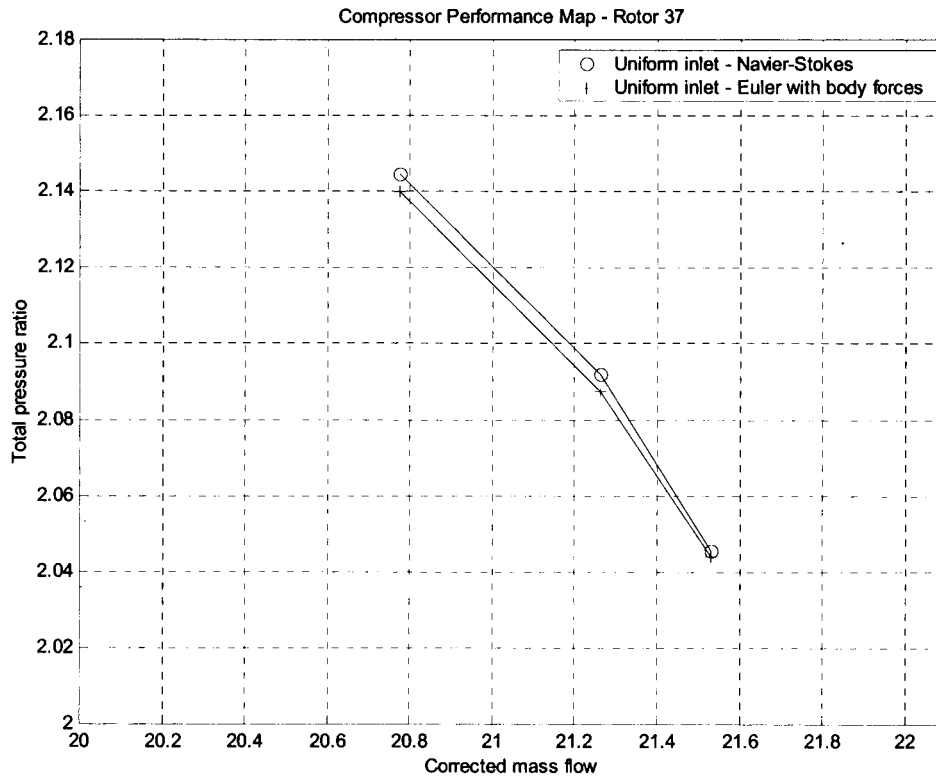


Figure 3.12: Comparisons of pressure-rise characteristics for three operating points from which the body-force database was generated

### 3.3 Radial Inlet Distortions

The steady state Euler solutions were obtained by applying the inflow and outflow boundary conditions constructed from the Navier-Stokes solutions with the radial inlet distortions. The converged solutions from operating point 4, shown in Figure 3.7, were selected as the initial conditions for this computation.

One-dimensional profiles that delineate the axial variations of the flow variables across the blade row are shown in Figure 3.13. It can be seen that the tangential velocity after the trailing edge was under-predicted by approximately 5 % of that from the Navier-Stokes

solutions. This also caused the total-pressure rise and the total-temperature rise to be approximately 1.0 % and 1.2 % less when compared to the total-pressure rise and the total-temperature rise computed from the Navier-Stokes solutions, respectively. Although the actual magnitudes of the static pressure and temperature near the inflow and outflow boundaries were differed from the Navier-Stokes solutions by a maximum of approximately 6 % of the static pressure at the exit, the pressure and temperature rises across the blade row were well predicted. In general, two-dimensional profiles in figure 3.14 to figure 3.16 also show good agreements, except near the end-wall boundaries.

The comparison of the pressure-rise characteristics subjected to the radial inlet distortions presented in Figure 3.17 indicates that the Euler computation with the body force formulation well captured the overall change of the rotor performance. The pressure-rise predicted by the body force formulation was found to be also less than that from the corresponding Navier-Stokes solutions by 1.2 % of the pressure-rise, exhibiting the same trend as in the uniform inlet cases.

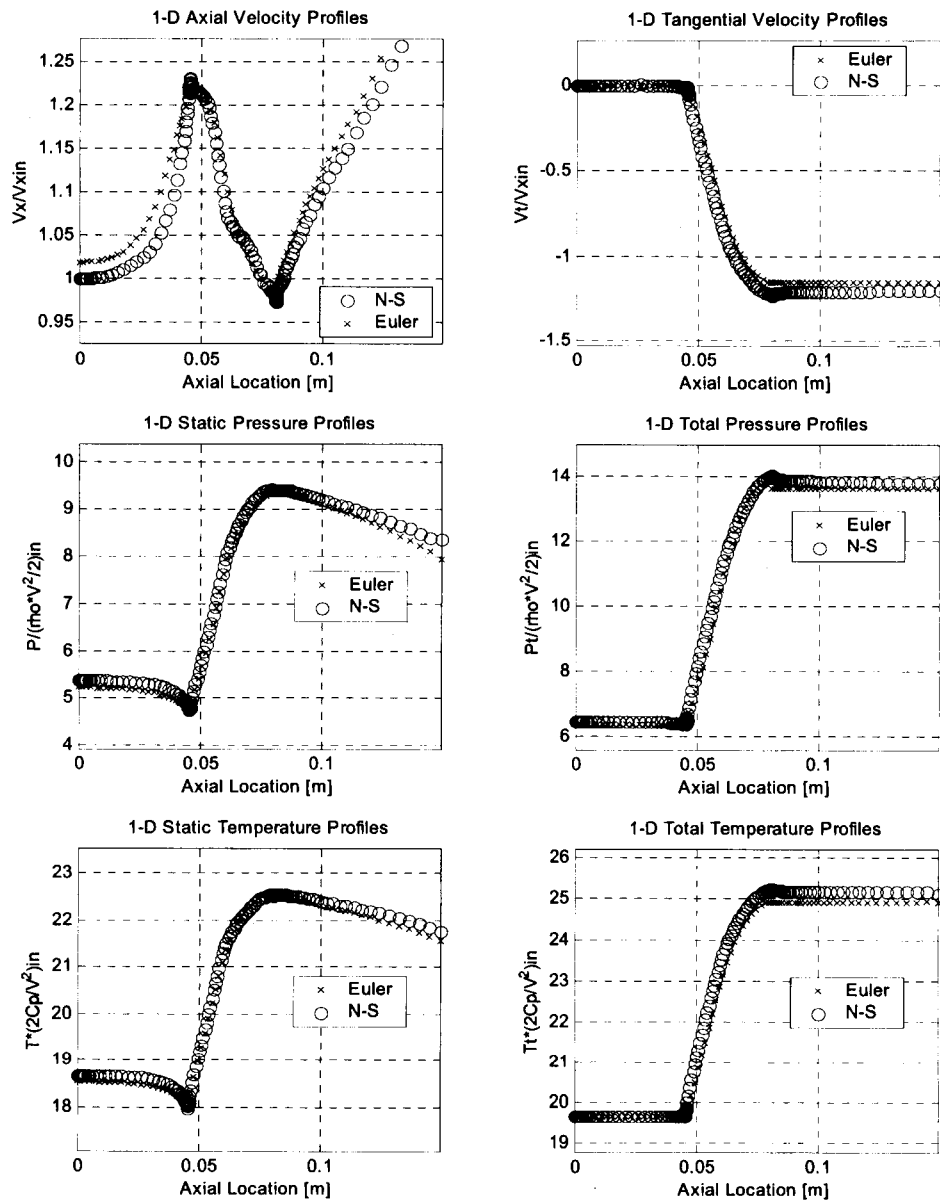


Figure 3.13: Comparisons of one-dimensional profiles of averaged flow solutions from the radial inlet distortion case. All quantities are mass averaged except axial velocity and static pressure for which area-averaging technique was used.

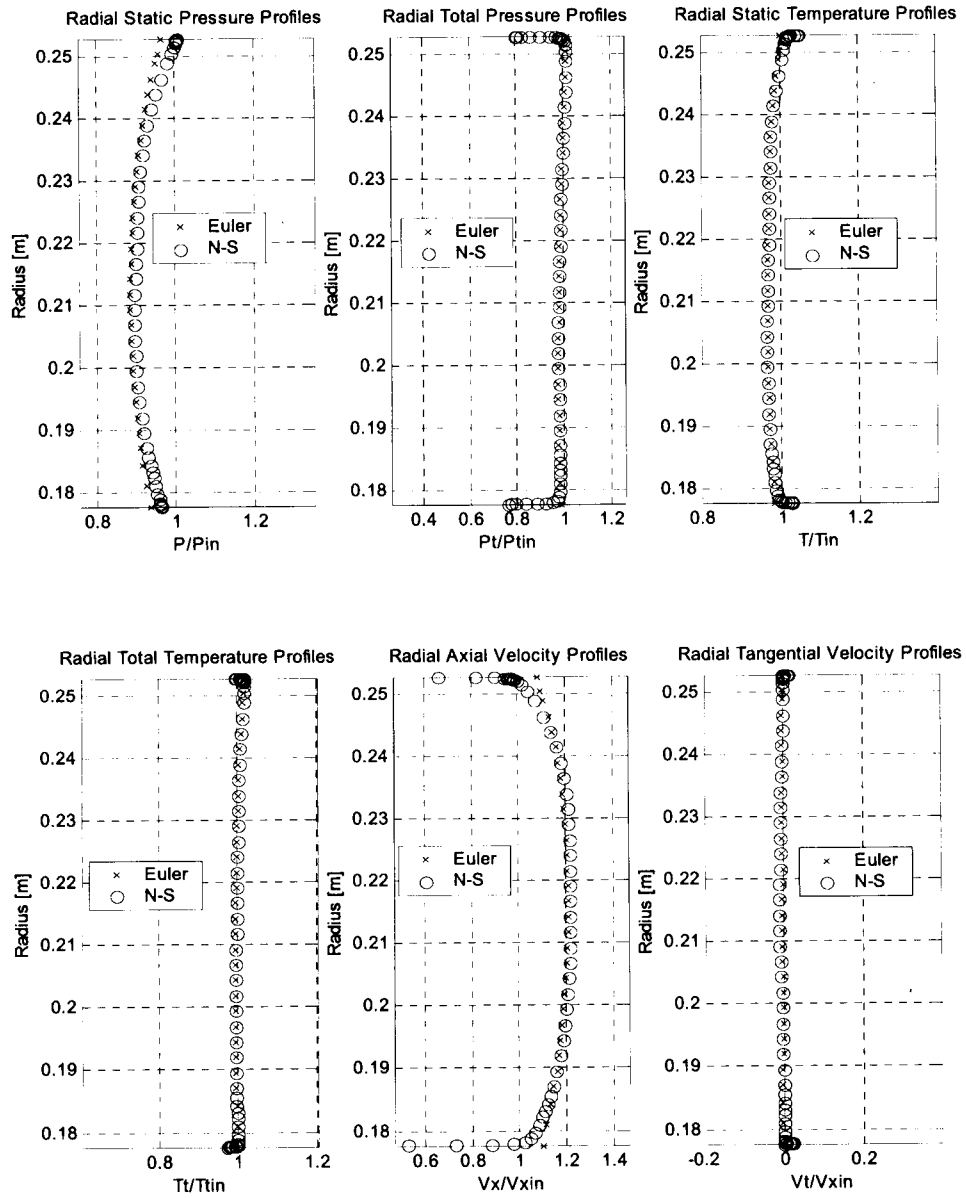


Figure 3.14: Comparisons of radial profiles prior to the leading edge from the radial inlet distortion case

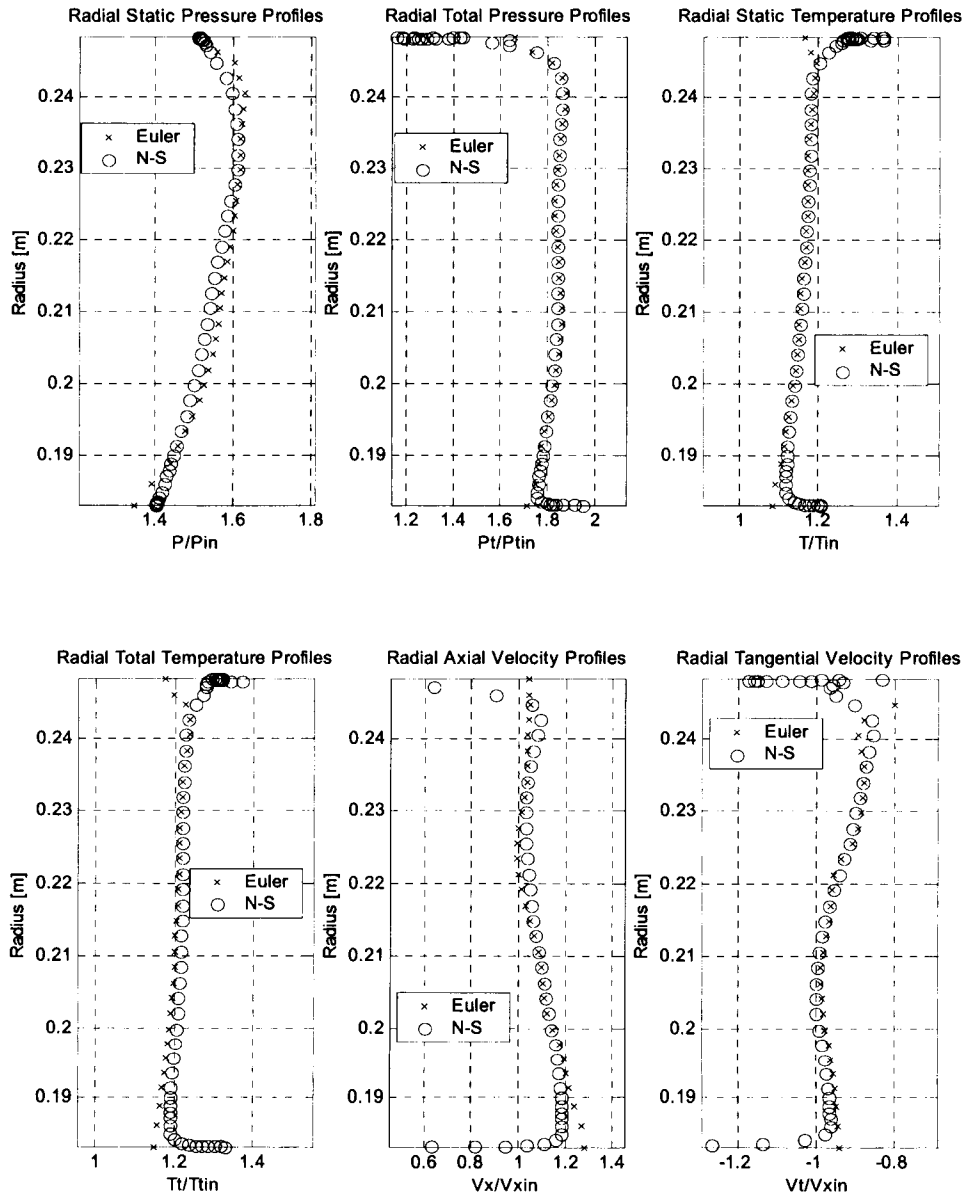


Figure 3.15: Comparisons of radial profiles at the mid-chord from the radial inlet distortion case

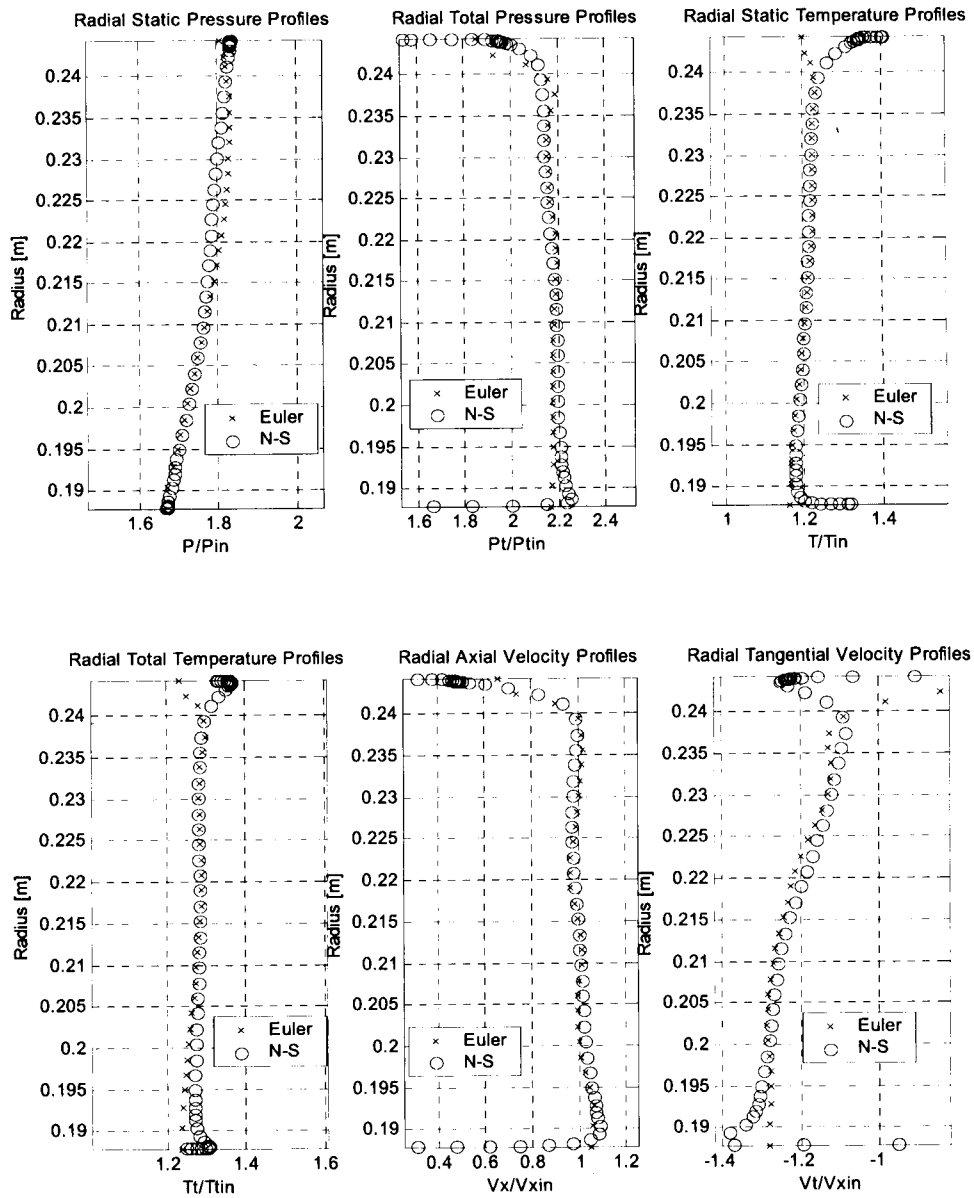


Figure 3.16: Comparisons of radial profiles after the trailing edge from the radial inlet distortion case

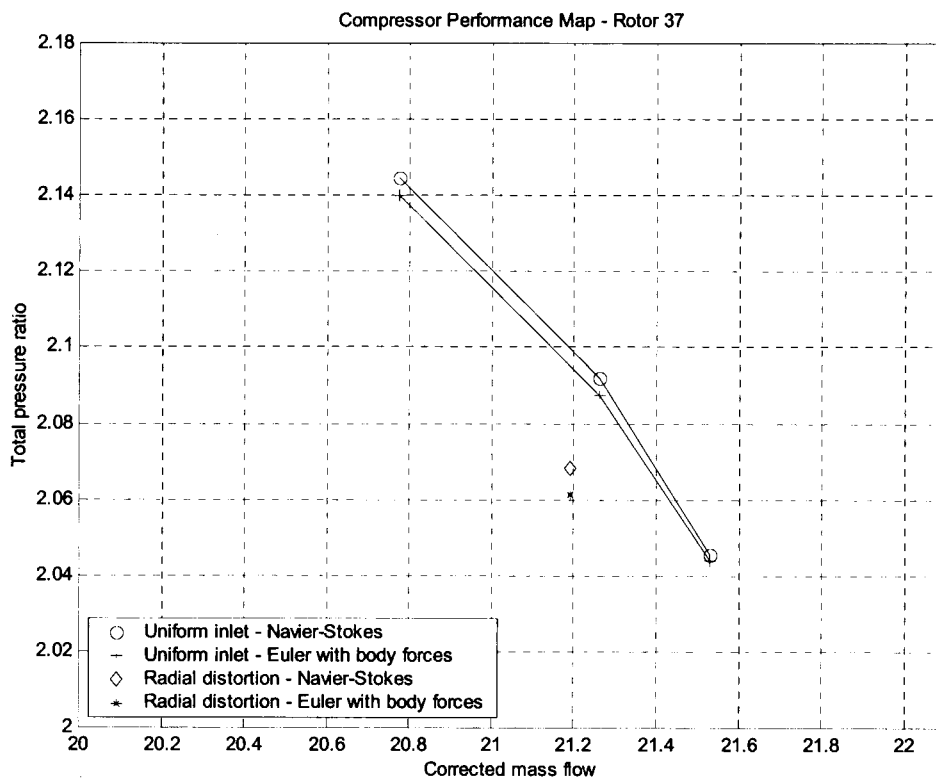


Figure 3.17: Comparisons of pressure-rise characteristics between the uniform inlet and radial inlet distortion cases

## **4. Summary and Concluding Remarks**

### **4.1 Summary**

The development of the computational methodology consists of using a few isolated-blade row Navier-Stokes solutions for each blade row to construct a body force database. The purpose of the body force database is to replace each blade row in a multi-stage compressor by a body force distribution to produce same pressure rise and flow turning. To do this, each body force database is generated in such a way that it can respond to the changes in local flow conditions and redistributes itself instantaneously. Once the database is generated, no further Navier-Stokes computations are necessary. The process is repeated for every blade row in the multi-stage compressor. Numerical predictions under a new set of inflow and outflow boundary and operating conditions can be carried out by using an Euler code with the body force databases.

The overall computational procedures for the concept validation as well as for the flow analysis with a body force database were developed. The corresponding body forces were embedded as source terms in the Euler equations.

A dimensional analysis was implemented to determine the local flow conditions that parameterize the magnitudes of the body forces. Three examples based on the use of the NASA Rotor 37 were presented to assess the physical consistency of the methodology. All the corresponding computational results from the test cases and their comparisons against the Navier-Stokes solutions are given in Section 3. Conclusions deduced from the computational results are provided in the next sub-section.

### **4.2 Concluding Remarks**

In general, the body forces can be parameterized in terms of the two relative flow angles, the relative Mach number and the Reynolds number when the flow relative to the blade is subsonic. For high-speed transonic flows, they can be parameterized in terms of local relative Mach number alone.

The physical consistency of the methodology developed here was demonstrated by the excellent agreements of both the one-dimensional variations and two-dimensional profiles of the flow quantities as well as the compressor performance obtained from the first example. The performance of a compressor blade row at a new operating point can be accurately predicted by using the body force database, which is created from the Navier-Stokes solutions with uniform inlet conditions. This capability was shown in the second example. The third example showed that the flow field subjected to radial inlet distortions could be predicted using the same body force database. The conclusions deduced from these three examples demonstrated the utility of the methodology for predicting the performance and the flow distribution in a multi-stage compressor.

### **4.3 Future Work**

While the results presented in this thesis are for a high-speed transonic blade row where the body forces can be parameterized in terms of the local relative Mach number, the application of the methodology to subsonic blade row will be demonstrated next. Here, the body forces will have to be parameterized in terms of the local relative Mach number, and the two local relative flow angles as well.

The radial profiles near the end-walls of a blade row can be improved by modeling the body forces created by the viscous effects, as shown in Figure 4.1, in the upstream region of the blade row. The implementation is relative simple and will be incorporated into the Euler code.

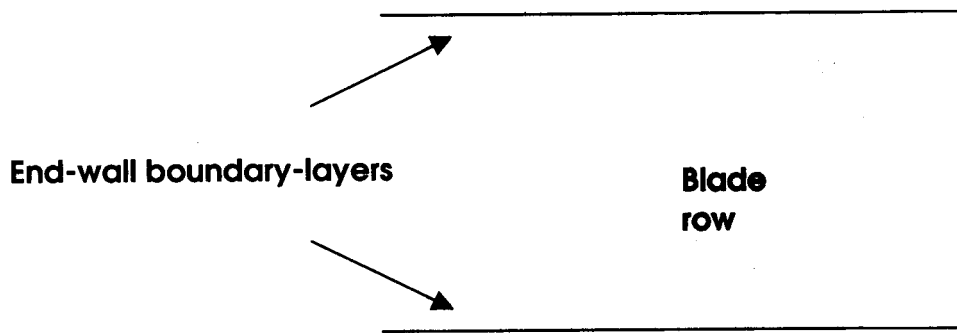


**Figure 4.1: End-wall boundary layer model**

## 5. REFERENCES

- [1] Gong, Y., Tan, C. S., Gordon, K. A., Greitzer, E. M., "A Computational Model for Short-wavelength Stall Inception and Development in Multistage Compressors," ASME JOURNAL OF TURBOMACHINERY, Vol. 121, 1999, pp. 726-734. Also Gong's doctoral thesis on "A Computational Model for Rotating Stall and Inlet Distortions in Multistage Compressors", 1999, Department of Aero. & Astro., MIT.
- [2] E. Hsiao, M. Naimi, J. P. Lewis, K. Dalbey, Y. Gong, C. Tan, "Actuator Duct Model of Turbomachinery Components for Powered-Nacelle Navier-Stokes Calculations," AIAA JOURNAL OF PROPULSION AND POWER, Vol. 17 No. 4 2001, pp. 919-927.
- [3] K. Suder, 1999, Private Communication.